Episodic diversifying selection and intragenomic interactions shape the evolution of DNA and RNA viruses

Stéphane Aris-Brosou[1,2,⋆] **Louis Parent,**[1] **and Neke Ibeh,**[1,†]

[1]Department of Biology, University of Ottawa, Ottawa, ON K1N 6N5, Canada

[2]Department of Mathematics and Statistics, University of Ottawa, Ottawa, ON K1N 6N5, Canada

[†]Current address: Princess Margaret Cancer Centre, the University Health Network, Toronto, ON M5G 2M9, Canada.

[⋆]**Corresponding author:** E-mail: `sarisbro@uottawa.ca`.

Abstract

Viruses are known to have some of the highest and most diverse mutation rates found in any biological replicator, topped by single-stranded (ss) RNA viruses, while double-stranded (ds) DNA viruses have rates approaching those of bacteria. As mutation rates are tightly and negatively correlated with genome size, selection is a clear driver of viral evolution. However, the role of intragenomic interactions as drivers of viral evolution is less well documented. To understand how these two processes affect viral evolution, we systematically surveyed ssRNA, ssDNA, dsRNA, and dsDNA viruses, to find which virus type and which functions show evidence for episodic diversifying selection and correlated evolution. We show that while evidence for selection is mostly found in single stranded viruses, and correlated evolution is more prevalent in DNA viruses, the genes that are affected by both processes are involved in key aspects of their life cycle, favoring viral stability over proliferation. We further show that both evolutionary processes are intimately linked at the amino acid level, which suggests that selection alone does not explain the whole evolutionary —and epidemiological— potential of viruses.

Keywords: correlated evolution, positive selection, adaptive evolution, gene ontology

Introduction

We are regularly reminded of the epidemiological toll of viruses, in part due to recent and ongoing viral outbreaks of influenza (Smith et al., 2009), Ebola (Gire et al., 2014), and Zika (Faria et al., 2016). Thanks to recent technological and analytical developments, it is now possible to elucidate, almost in real time (Faria et al., 2016), their epidemiological dynamics, and unravel their evolutionary dynamics (Grenfell et al., 2004). However, while the evolutionary dynamics of RNA viruses are well documented (Holmes, 2009), those of other viruses are not so well known, in particular in a unifying context including major viral types such as double-stranded (ds) and single-stranded (ss) DNA and RNA viruses.

To date, one of the most salient evolutionary features shared by all viruses is the existence of a negative correlation between mutation rate and genome size (*e.g.*, Holmes, 2009). This is a critical result as it suggests that selection is driving the evolution of mutation rates, establishing a tradeoff between mutational load and availability of adaptive mutations (Holmes, 2011). But the processes driving the evolution of different types of viruses are multiple. As already argued, both ssDNA and ssRNA viruses share small genome sizes, high mutation rates, but also large effective population sizes, little to no gene duplication or recombination, and overlapping reading frames (Holmes, 2009). This last point suggests that a seldom explored evolutionary process, correlated evolution, might play a key role in the evolution of these single-stranded viruses. Indeed, recent work uncovered pervasive evidence for correlated evolution in influenza viruses (Nshogozabahizi et al., 2017), and both the Zika (Aris-Brosou et al., 2017) and the Ebola viruses (Ibeh et al., 2016), with evidence in the latter that sites evolving in a correlated manner can also be under episodic diversifying selection. However, this recent body of evidence is so far limited to a small number of ssRNA viruses, so that the combined role of correlated

evolution and selection is difficult to generalize.

To better understand the role of correlated evolution and selection in the evolutionary dynamics of viruses, we constructed a nearly exhaustive viral data set spanning all dsDNA, dsRNA, ssRNA, and ssDNA viruses deposited in GenBank (as of August 2017), and conducted an extensive survey of correlated evolution and diversifying selection in these viruses, asking more specifically about the prevalence of these two processes in each viral type, independently or jointly, with the specific hypothesis that the genes affected by both processes encode functions that are most critical to each viral life cycle.

Results and Discussion

First, in order to better understand the genomic characteristics of the four types of viruses, dsDNA, dsRNA, ssRNA, and ssDNA, and understand how these characteristics can impact the evolutionary dynamics of these viruses (Methods; Figure S1), we examined the distribution of four of their genomic features. While dsDNA viruses had the largest and the most variable genome lengths, ssDNA were the smallest genomes by at least an order of magnitude, with both dsRNA and ssRNA exhibiting intermediate sizes (Figure 1a). Because of the compact structure of these genomes, these differences were also reflected in the number of genes, protein-coding genes, and RNAs encoded by the genomes of these viruses (Figure S2). In turn, these characteristics suggest that with their large genomes, dsDNA viruses potentially have a higher degree of functional redundancy than ssDNA or even ssRNA viruses, possibly due to duplication events (Gao et al., 2017), and thereby be under less stringent selective pressures than viruses with smaller genomes. On the other hand, the extent of correlated evolution and its interaction with selection is more difficult to predict.

To address these questions, we first tested for the presence of episodic diversifying selection in each viral type. Altogether, we found extensive differences among all four viral types (Figure 1b; $X^2 = 99.61$, $df = 3$, $P < 2.2 \times 10^{-16}$), and that single stranded viruses were more subject to selection than double stranded viruses ($X^2 = 95.14$, $df = 1$, $P < 2.2 \times 10^{-16}$). Indeed, and *contra* our original hypothesis, there were no differences between dsDNA and dsRNA viruses ($X^2 = 0.26$, $df = 1$, $P = 0.6110$), or between ssDNA and ssRNA viruses in terms of prevalence of diversifying selection ($X^2 = 2.07$, $df = 1$, $P = 0.1503$). However, it is unlikely that "strandedness" (single *vs.* double stranded genetic material) alone drives selection, even if greater instability can be postulated in single-stranded nucleic acids (Frederico et al., 1990). Indeed, strandedness is negatively correlated with genome size ($t = -4.98$, $df = 108.35$, $P = 2.43 \times 10^{-6}$), which is itself correlated with mutation rates (*e.g.* Lynch, 2007; Duffy, 2018). As a result, episodic diversifying selection is mostly driven by structural aspects of viral genomes, that condition mutation rates across all virus types (Sanjuán, 2012).

To understand if similar aspects drive intragenic correlated evolution, we counted in the same way the number of genes for which we could find evidence for interactions. Here again, we found extensive differences among all four viral types (Figure 1c; $X^2 = 29.79$, $df = 3$, $P < 1.5 \times 10^{-16}$), with no difference between dsDNA and ssDNA viruses ($X^2 = 0.0005$, $df = 1$, $P = 0.9827$), or between dsRNA and ssRNA viruses ($X^2 = 0.0001$, $df = 3$, $P = 0.9903$). As a result, the prevalence of correlated evolution is mostly driven by the nature of viral genetic material. At least two processes can underpin correlated evolution: linkage and epistasis (Dench et al., 2018). As recombination is pervasive in some dsDNA viruses (Robinson et al., 2011), linkage alone may not explain the high prevalence of correlated evolution in DNA viruses (close to 40%: Figure 1c). Rather, this pattern suggests that intragenic constraints are higher in DNA viruses for unknown

structural reasons, maybe due to protein structure (Woo et al., 2014), or in the same way that recombination in RNA viruses may be driven by mechanistic constraints associated with genome structures and viral life cycles (Simon-Loriere and Holmes, 2011) .

While previous work showed that both diversifying selection and correlated evolution can affect the same gene and even the same site in a viral genome such as Ebola's (Ibeh et al., 2016), a ssRNA virus, the generality of this association is still unknown. At the gene level, we found strong heterogeneity among all four viral types for gene numbers showing evidence for selection, correlated evolution or both ($X^2 = 206.54$, $df = 6$, $P < 2.2 \times 10^{-16}$). Surprisingly, ssRNA viruses are those that show the least overlap between selection and correlated evolution, with only 11% of the genes evolving under both mechanisms (Figure 1d). Patterns are however much more difficult to extract here, mostly because the number of genes involved becomes quite small, in particular for the virus type with most overlap, the dsRNA viruses (Figure 1d: 29.4%, *i.e.* five genes).

To assess the extent to which some of these differences at the gene level are functionally driven, we extracted the Gene Ontology (GO) annotations, or GO terms, associated with the genes analyzed, as well as those under selection, correlated evolution, or both – focusing exclusively on the virus types for which we had the largest samples sizes, dsDNA and ssRNA viruses (Figure 1e). Each of the three parts of the ontology (Molecular Function [MF], Biological Process [BP], and Cellular Component [CC]) were first limited to the second level of GO. Figure 1e shows that GO terms related to catalytic activity (MF), involved in the establishment or maintenance of a certain location (BP) at the membrane level (CC) are predominantly present in both dsDNA and ssRNA genomes. However, only a subset of these GO terms are overrepresented: helicase activity / binding (MF) and replication (BP) in the host cell nucleus (CC) are mostly under episodic diversifying selection in dsDNA, while it is mostly peptidase activity and methylation on

the viral envelope for ssRNA viruses (Table S1; $P < 0.01$). Helicase activity and binding at the interface of multiple compartments are also overrepresented as being involved in correlated evolution for dsDNA viruses, while it is transferase activity and protein modifications on the envelope for ssRNA viruses (Table S2). At the intersect of both processes, episodic diversifying selection and correlated evolution, the key GO terms focus on structural integrity of a complex or its assembly within or outside a cell at the capsid level for dsDNA viruses, while they do focus on interactions with host cell surface via antigen activity on the viral envelope for ssRNA viruses (Table 3). This suggests key differences in life history strategies adopted by these two types of viruses, with capsid assembly (dsDNA) and host cell interaction (ssRNA) being the most critical aspects of their evolutionary biology. Indeed, previous work highlighted the existence of tradeoffs between capsid stability and proliferation within a host (De Paepe and Taddei, 2006), or fecundity and lifespan (García-Villada and Drake, 2013) in dsDNA viruses, which supports the idea that selection and correlated evolution can shape viral life histories.

The previous analyses were at the gene level. One outstanding question is whether this relationship between selection and correlated evolution also holds at the amino acid level. This question was addressed in two different ways, all virus types confounded (in order to have larger sample sizes), by focusing on one process at a time, and finding at what point evidence supporting the second process becomes significant. First, we searched the list of pairs of sites evolving in a correlated manner (the SM sites) to see if at least one pair member was potentially evolving under episodic diversifying selection (the MEME sites), irrespective of its probability of being a MEME site. For this, we identified pairs of SM sites, that is those with a posterior probability ≥ 0.95, and plotted their posterior probability as a function of the $-\log_{10}$ probability of each pair member to be under selection (Figure 2a). Both the least-square ($\hat{\rho}_{\text{slope}} = 0.005$, $t = 3.90$, $P = 0.0001$) and

the robust regressions ($\hat{\rho}_{\text{slope}} = 0.005$, $t = 2.62$, $P = 0.0089$) have positive and significant slopes, hereby demonstrating the existence of a relationship between correlated evolution and episodic diversifying selection at the amino acid level – even if most of the SM sites show weak evidence of selection (at $P \leq 0.01$, gray broken line in Figure 2a). So, to validate the existence of this relationship, we then took the list of MEME sites, and searched the list of SM sites to see if at least one pair member was potentially a MEME site, irrespective of its posterior probability of being in an SM site pair. For this, we identified the MEME sites, that is those with a P-value ≤ 0.01 (≥ 2 on a $-\log_{10}$ scale), and plotted this (on the x-scale) *vs.* their posterior probability of being in an SM pair (on the y-scale; Figure 2b). Both the least-square ($\hat{\rho}_{\text{slope}} = 0.026$, $t = 3.64$, $P = 0.0003$) and the robust regressions ($\hat{\rho}_{\text{slope}} = 0.031$, $t = 3.37$, $P = 0.0008$) have positive and significant slopes, further confirming the existence of a relationship between correlated evolution and episodic diversifying selection at the amino acid site level. Note however that this latter analysis is more informative than the former, as the density also shows that most of the sites under selection are involved in weak interactions. This is intriguingly reminiscent of the involvement of weakly interacting pairs of sites in severe outbreaks or pandemics (Aris-Brosou et al., 2017).

Altogether, this work shows that while episodic diversifying selection is mostly found in single stranded viruses and correlated evolution is more prevalent in DNA viruses, both evolutionary processes may shape the life history of viruses, favoring stability over proliferation, and that ultimately, selection and correlated evolution are intimately linked at the amino acid level. However, we neglected some aspects of viral structure: indeed, viruses can be segmented or not, with a circular or linear genome, with positive or negative strands, complications that we did not consider here, and which could impact the mode of evolution of viruses (Holmes, 2009). We also neglected the population genetics context

in which different viruses evolve, and these are often correlated to structural constraints (Lynch, 2007; Holmes, 2009). Furthermore, as we solely focused on intragenic interactions, and not intergenic or higher order correlations, it is not impossible that we missed higher-level constraints affecting viral evolution. In particular, it is possible that intergenic correlations reveal the nature of tradeoffs shaping the life history strategies in viruses (De Paepe and Taddei, 2006). Future modeling (Neverov et al., 2015) and empirical (Ashenberg et al., 2017) work should probably focus on elucidating these constraints.

Methods

Data retrieval

Lists of dsDNA, dsRNA, ssRNA, and ssDNA viruses infecting humans were retrieved from the viruSITE database (Stano et al., 2016) in August 2017. Each list contained the virus names, the length of their genome, their number of protein-coding genes (CDS's), and was associated with a reference coding sequence. In order to obtain corresponding sequence alignments of orthologous genes, BLASTn searches were performed on a custom database limited to viral genes present in NCBI nucleotide database with blast-2.6.0+. For this, all gbvrl*.seq.gz files were downloaded from `ftp.ncbi.nih.gov/genbank` while querying viruSITE, and were concatenated into a single GenBank file, then converted into a FASTA file with `readseq` to specifically extract CDS's (Gilbert, 2003). This was done to avoid retrieving 5' and 3' untranslated regions that would cause problems to the downstream codon analyses. BLASTn searches were performed for each viruSITE viral sequence with a stringent E-value threshold of 10^{-100}, keeping a maximum of 100 sequences with at least 80% coverage with each query. Only data sets with at least 20 hits were kept for downstream analyses. Sequences corresponding to each accession number

were retrieved from the FASTA file obtained with `readseq` (Gilbert, 2003).

Because this file contained partial sequences, each set of retrieved sequences was first aligned with `Muscle` 3.8.31 (Edgar, 2004). Each alignment was then quality checked ensuring that (i) its length is a multiple of three, (ii) it starts with an ATG and stops with a stop codon. Alignments failing at least one condition were discarded. Within each alignment, mean numbers of indels $\hat{n}_{indels}$ were computed for each sequence, and those containing number of indels $\geq \hat{n}_{indels} + 1SEM$ were eliminated. The remaining nucleotide sequences were then re-aligned with TranslatorX (Abascal et al., 2010), at the amino acid level, using the `Muscle` aligner and their heuristics to determine the correct reading frame. Alignment files were then cleaned-up with `Gblocks` 0.91b at the codon level using the stringent default settings (Castresana, 2000).

Gene Ontology (GO) terms were retrieved from gene sequences with HMMER2GO (`github.com/sestaton/HMMER2GO`), relying on the Hidden Markov Models in `ftp.ebi.ac.uk/pub/databases/Pfam/current_release/Pfam-A.hmm.gz` (ver. Feb 23, 2017). Individual mapping files coming from our four viral types (sRNA, dsRNA, ssDNA, and dsDNA viruses) were then merged to create a custom annotation file, used for GO term enrichment testing with topGO (Alexa and Rahnenführer, 2009), based on Fisher's exact test. The reference gene list was always the entire set of genes within each viral type.

Phylogenetic analyses

Phylogenetic trees were reconstructed with `FastTree` 2.1.7 (Price et al., 2010) under the GTR $+\Gamma$ model of evolution (*e.g.,* Aris-Brosou and Rodrigue, 2012). Those with a nonzero tree length were midpoint rerooted using the phytools package ver. 0.4-60 (Revell, 2012) in R ver. 3.2.3 (R Core Team, 2016).

Patterns of correlated evolution among sites were identified with the Bayesian graphi-

cal model (BGM) implemented in SpiderMonkey (Poon et al., 2008), which is part of HyPhy ver. 2.3.3 (Pond et al., 2005). Default HyPhy scripts were slightly modified to read in codon data, which were used to reconstruct mutational paths under the MG94×HKY85 substitution model (Kosakovsky Pond and Frost, 2005) at non-synonymous sites along each branch of the estimated trees. Ambiguous reconstructions were resolved by considering all possible resolutions and averaging them. These reconstructed mutational paths were then recoded as a binary matrix, with rows corresponding to branches and columns to a site of the alignment. The BGM was then used to identify the pairs of sites that exhibit correlated patterns of non-substitutions according to their posterior probability, estimated with a Markov chain Monte Carlo sampler that was run for 10^5 steps, with a burn-in period of 10,000 steps sampling every 1,000 steps for inference (see also: Aris-Brosou et al., 2017).

Patterns of episodic selection were identified based on the Mixed Effects Model of Evolution (MEME; Murrell et al., 2012), also as implemented in HyPhy. The default script from ver. 2.2.6 was used, still with the 2.3.3 HyPhy engine, to infer non-synonymous to synonymous rate ratios ω assuming that these rates can vary across lineages and among sites. In this implementation, two categories of sites were assumed, those for which $\omega_{neg} \leq 1$, in proportion p, and those for which $\omega_{pos} > 1$, that are under positive selection, in proportion $1 - p$. Evidence for selection was derived by means of a likelihood ratio test between this model, and a null model where ω_{pos} was constrained to take its value between 0 and 1. All alignments and scripts are available from `https://github.com/sarisbro`.

Acknowledgements

We thank Compute Canada and Ontario's Center for Advanced Computing for giving us access to their servers. This work was supported by the Natural Sciences Research Council of Canada (SAB), and by the University of Ottawa (LP, NI).

References

Abascal F, Zardoya R, Telford MJ. 2010, Jul. TranslatorX: multiple alignment of nucleotide sequences guided by amino acid translations. Nucleic Acids Res. 38(Web Server issue):W7–13.

Alexa A, Rahnenführer J. 2009. Gene set enrichment analysis with topgo. Bioconductor Improv. 27.

Aris-Brosou S, Ibeh N, Noël J. 2017, Sep. Viral outbreaks involve destabilized evolutionary networks: evidence from ebola, influenza and zika. Sci Rep. 7(1):11881.

Aris-Brosou S, Rodrigue N. 2012. The essentials of computational molecular evolution. Methods Mol Biol. 855:111–52.

Ashenberg O, Padmakumar J, Doud MB, Bloom JD. 2017, 03. Deep mutational scanning identifies sites in influenza nucleoprotein that affect viral inhibition by mxa. PLoS Pathog. 13(3):e1006288.

Castresana J. 2000. Selection of conserved blocks from multiple alignments for their use in phylogenetic analysis. Molecular biology and evolution. 17(4):540–552.

De Paepe M, Taddei F. 2006, Jul. Viruses' life history: towards a mechanistic basis of a trade-off between survival and reproduction among phages. PLoS Biol. 4(7):e193.

Dench J, Aris-Brosou S, Kassen R. 2018. The idiosyncratic drivers of correlated evolution. bioRxiv.:474536.

Duffy S. 2018, Aug. Why are rna virus mutation rates so damn high? PLoS Biol. 16(8):e3000003.

Edgar RC. 2004. Muscle: multiple sequence alignment with high accuracy and high throughput. Nucleic acids research. 32(5):1792–1797.

Faria NR, Azevedo RdSdS, Kraemer MUG, Souza R, Cunha MS, Hill SC, Thézé J, Bonsall MB, Bowden TA, Rissanen I, Rocco IM, Nogueira JS, Maeda AY, Vasami FGdS, Macedo FLdL, Suzuki A, Rodrigues SG, Cruz ACR, Nunes BT, Medeiros DBdA, Rodrigues DSG, Queiroz ALN, da Silva EVP, Henriques DF, da Rosa EST, de Oliveira CS, Martins LC, Vasconcelos HB, Casseb LMN, Simith DdB, Messina JP, Abade L, Lourenço J, Alcantara LCJ, de Lima MM, Giovanetti M, Hay SI, de Oliveira RS, Lemos PdS, de Oliveira LF, de Lima CPS, da Silva SP, de Vasconcelos JM, Franco L, Cardoso JF, Vianez-Júnior JLdSG, Mir D, Bello G, Delatorre E, Khan K, Creatore M, Coelho GE, de Oliveira WK, Tesh R, Pybus OG, Nunes MRT, Vasconcelos PFC. 2016*a*, Apr. Zika virus in the americas: Early epidemiological and genetic findings. Science. 352(6283):345–349.

Faria NR, Sabino EC, Nunes MRT, Alcantara LCJ, Loman NJ, Pybus OG. 2016*b*, Sep. Mobile real-time surveillance of zika virus in brazil. Genome Medicine. 8(1).

Frederico LA, Kunkel TA, Shaw BR. 1990, Mar. A sensitive genetic assay for the detection of cytosine deamination: determination of rate constants and the activation energy. Biochemistry. 29(10):2532–7.

Gao Y, Zhao H, Jin Y, Xu X, Han GZ. 2017. Extent and evolution of gene duplication in DNA viruses. Virus research. 240:161–165.

García-Villada L, Drake JW. 2013, Jun. Experimental selection reveals a trade-off between fecundity and lifespan in the coliphage qß. Open Biol. 3(6):130043.

Gilbert D. 2003, Feb. Sequence file format conversion with command-line readseq. Curr Protoc Bioinformatics. Appendix 1:Appendix 1E.

Gire SK, Goba A, Andersen KG, Sealfon RSG, Park DJ, Kanneh L, Jalloh S, Momoh M, Fullah M, Dudas G, Wohl S, Moses LM, Yozwiak NL, Winnicki S, Matranga CB, Malboeuf CM, Qu J, Gladden AD, Schaffner SF, Yang X, Jiang PP, Nekoui M, Colubri A, Coomber MR, Fonnie M, Moigboi A, Gbakie M, Kamara FK, Tucker V, Konuwa E, Saffa S, Sellu J, Jalloh AA, Kovoma A, Koninga J, Mustapha I, Kargbo K, Foday M, Yillah M, Kanneh F, Robert W, Massally JLB, Chapman SB, Bochicchio J, Murphy C, Nusbaum C, Young S, Birren BW, Grant DS, Scheiffelin JS, Lander ES, Happi C, Gevao SM, Gnirke A, Rambaut A, Garry RF, Khan SH, Sabeti PC. 2014, Sep. Genomic surveillance elucidates ebola virus origin and transmission during the 2014 outbreak. Science. 345(6202):1369–72.

Grenfell BT, Pybus OG, Gog JR, Wood JLN, Daly JM, Mumford JA, Holmes EC. 2004, Jan. Unifying the epidemiological and evolutionary dynamics of pathogens. Science. 303(5656):327–32.

Holmes EC. 2009. The evolution and emergence of RNA viruses. Oxford series in ecology and evolution. Oxford: Oxford University Press.

Holmes EC. 2011, Jun. What does virus evolution tell us about virus origins? J Virol. 85(11):5247–51.

Ibeh N, Nshogozabahizi JC, Aris-Brosou S. 2016, 06. Both epistasis and diversifying selection drive the structural evolution of the ebola virus glycoprotein mucin-like domain. J Virol. 90(11):5475–5484.

Kosakovsky Pond SL, Frost SDW. 2005, May. Not so different after all: a comparison of methods for detecting amino acid sites under selection. Mol Biol Evol. 22(5):1208–22.

Lynch M. 2007. The origins of genome architecture. Sunderland, Mass.: Sinauer Associates.

Murrell B, Wertheim JO, Moola S, Weighill T, Scheffler K, Kosakovsky Pond SL. 2012. Detecting individual sites subject to episodic diversifying selection. PLoS Genet. 8(7):e1002764.

Neverov AD, Kryazhimskiy S, Plotkin JB, Bazykin GA. 2015, Aug. Coordinated evolution of influenza a surface proteins. PLoS Genet. 11(8):e1005404.

Nshogozabahizi JC, Dench J, Aris-Brosou S. 2017, 01. Widespread historical contingency in influenza viruses. Genetics. 205(1):409–420.

Pond SLK, Frost SDW, Muse SV. 2005, Mar. Hyphy: hypothesis testing using phylogenies. Bioinformatics. 21(5):676–9.

Poon AFY, Lewis FI, Frost SDW, Kosakovsky Pond SL. 2008, Sep. Spidermonkey: rapid detection of co-evolving sites using bayesian graphical models. Bioinformatics. 24(17):1949–50.

Price MN, Dehal PS, Arkin AP. 2010, Mar. FastTree 2–approximately maximum-likelihood trees for large alignments. PLoS One. 5(3):e9490.

R Core Team. 2016. R: A Language and Environment for Statistical Computing. R Foundation for Statistical Computing, Vienna, Austria.

Revell LJ. 2012. phytools: an R package for phylogenetic comparative biology (and other things). Methods in Ecology and Evolution. 3(2):217–223.

Robinson CM, Seto D, Jones MS, Dyer DW, Chodosh J. 2011, Aug. Molecular evolution of human species D adenoviruses. Infect Genet Evol. 11(6):1208–17.

Sanjuán R. 2012. From molecular genetics to phylodynamics: evolutionary relevance of mutation rates across viruses. PLoS Pathog. 8(5):e1002685.

Simon-Loriere E, Holmes EC. 2011, Jul. Why do RNA viruses recombine? Nat Rev Microbiol. 9(8):617–26.

Smith GJD, Vijaykrishna D, Bahl J, Lycett SJ, Worobey M, Pybus OG, Ma SK, Cheung CL, Raghwani J, Bhatt S, Peiris JSM, Guan Y, Rambaut A. 2009, Jun. Origins and evolutionary genomics of the 2009 swine-origin h1n1 influenza a epidemic. Nature. 459(7250):1122–5.

Stano M, Beke G, Klucar L. 2016. viruSITE-integrated database for viral genomics. Database (Oxford). 2016.

Woo J, Robertson DL, Lovell SC. 2014, Apr. Constraints from protein structure and intra-molecular coevolution influence the fitness of hiv-1 recombinants. Virology. 454-455:34–9.

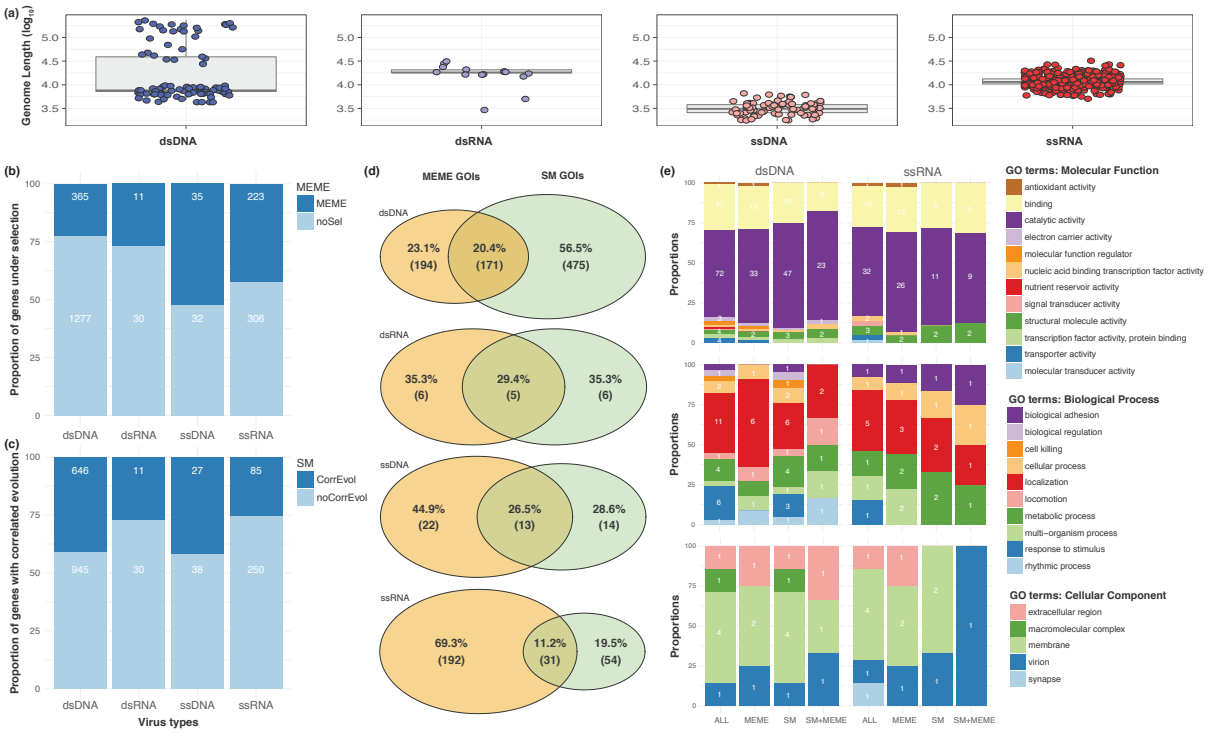

Figure 1. Modes of evolution of viruses. (a) Distribution of genome size, on a $\log_{10}$ scale ssRNA (blue), ssDNA (purple), dsRNA (orange), and dsDNA (red). **(b)** Proportion of genes detected to be under diversifying selection (top, dark hues); actual numbers of genes are shown within each column. **(c)** Proportion of genes detected to be evolving in a correlated manner (top, dark hues); actual numbers of genes are shown within each column. **(d)** Venn diagrams showing the Genes of Interest (GOIs) either under selection (MEME GOIs), or evolving in a correlated manner (SM GOIs), or both (intersect) for each virus type. **(e)** Gene Ontology (GO) enrichment tests for the genes that are both under selection and evolving in a correlated manner for their Molecular Function (top), Biological Processes (middle), and Cellular Component (bottom), all at level 2 of the ontology.

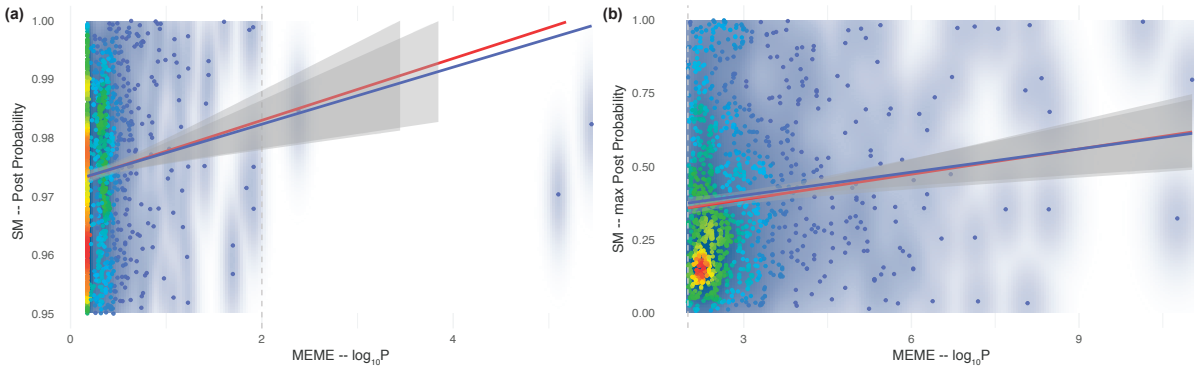

Figure 2. Strength of evidence for sites under both selection (MEME) and correlated evolution (SM). (a) SM sites that are also under episodic diversifying selection. **(b)** MEME sites that are also evolving in a correlated manner. In both cases, the posterior probability of a site evolving in a correlated manner is plotted as a function of the P-value of a site being under selection (on a $-\log_{10}$ scale). Regular least-square regressions are shown in blue; robust regressions are shown in red; 95% confidence envelopes are shaded in gray. See text for statistical details. Density scale: from low (cool colors) to high (warm colors).